Syntheses and Structural Characterizations of Sheet- and Column-like Lanthanide−Transition Metal Arrays: The Effect of Hydrogen Bonding on the Structure When K^+ Is Replaced by $[NH_4]^+$

Bin Du, Edward A. Meyers, and Sheldon G. Shore*

Evans Laboratory, Department of Chemistry, The Ohio State University, Columbus, Ohio 43210

Received December 29, 2000

Sheet- and column-like cyanide bridged lanthanide−transition metal arrays were synthesized through metathesis reactions between anhydrous $LnCl_3$ (Ln = Eu, Yb) and $A_2[M(CN)_4]$ (A = K^+, NH_4^+; M = Ni, Pt) in a 1:2 molar ratio in DMF (DMF = *N*,*N*-dimethylformamide) solution. Single-crystal X-ray analysis revealed that complexes of formula $\{K(DMF)_7Ln[M(CN)_4]_2\}_\infty$ (Ln = Eu, M = Ni, **1**; Ln = Yb, M = Pt, **2**) consist of infinite layers of neutral, puckered sheets that contain hexagonal rings of composition $\{(DMF)_{10}Ln_2[M(CN)_4]_3\}_6$ with interstitial $(DMF)_4K_2[M(CN)_4]$ units located between the layers. The sheet structure is generated through the repeating $(DMF)_{10}Ln_2[M(CN)_4]_3$ unit with trans cyanide ligands in $[M(CN)_4]^{2-}$ serving as bridges. The column-like complex $\{(NH_4)(DMF)_4Yb[Pt(CN)_4]_2\}_\infty$, **3**, is formed when NH_4^+ replaces K^+. It consists of infinite, negatively charged, square, parallel columns bundled through N−H···NC hydrogen bonds between NH_4^+ and terminal CN from the columns. Cis cyanide ligands in $[Pt(CN)_4]^{2-}$ units serve as bridges. Complex **3** is the first known example where Ln(III) centers are coordinated to four $[M(CN)_4]^{2-}$ units. Bicapped (square face) trigonal prismatic coordination geometries were observed for Ln(III) centers in **1** and **2**. Square antiprismatic geometry for Yb(III) centers are observed in **3**. Crystal data for **1**: triclinic space group $P\bar{1}$, $a = 8.797(2)$ Å, $b = 15.621(3)$ Å, $c = 17.973(6)$ Å, $\alpha = 105.48(2)°$, $\beta = 98.60(2)°$, $\gamma = 98.15(2)°$, $Z = 2$. Crystal data for **2**: triclinic space group $P\bar{1}$, $a = 8.825(1)$ Å, $b = 15.673(1)$ Å, $c = 17.946(1)$ Å, $\alpha = 105.46(2)°$, $\beta = 99.10(1)°$, $\gamma = 98.59(1)°$, $Z = 2$. Crystal data for **3**: monoclinic space group $P2_1/c$, $a = 9.032(1)$ Å, $b = 29.062(1)$ Å, $c = 15.316(1)$ Å, $\beta = 94.51(1)°$, $Z = 2$.

Introduction

We are interested in synthesizing cyanide-bridged lanthanide−transition metal arrays with a view toward systematizing synthetic procedures and categorizing structures of the types of arrays that are formed.[1] The study of complexes that contain both a lanthanide and a transition metal is not only of intrinsic interest, but increasingly such systems offer possibilities for various applications. We have previously cited some of these applications.[2] In this respect, we are concerned with the application of cyanide-bridged lanthanide−transition metal complexes as precursors for the formation of bimetallic catalysts for heterogeneous catalytic reactions in which the lanthanide enhances the catalytic activity. Accordingly, we have observed that the resistance to oxidation of Pd in the catalytic reduction of NO by methane in the presence of oxygen is enhanced when the Pd is in intimate contact with Yb or Sm.[3] We are also interested in and have studied the magnetic properties of selected multidimensional array cyanide-bridged lanthanide−transition metal complexes including the complexes described here,[4] since higher dimensionality is required in order for a complex to achieve long-range magnetic ordering at finite temperature.[5]

Previously, we reported two series of cyanide-bridged lanthanide−transition metal extended arrays of general composition $\{(DMF)_{10}Ln_2[M(CN)_4]_3\}_4$ where Ln(III) = Eu, Sm, Er, Yb, Y; M(II) = Ni, Pd, Pt; DMF = *N*,*N*-dimethylformamide. These complexes are one-dimensional extended single-strand (type **A**) or double-strand (type **B**) linear arrays in the solid state.[1b,d,h] These types have the same repeating unit. They are formed in the absence of water. In the presence of water, either oligomeric structures or zigzag chain structures are formed.[1g,4a] We report here syntheses and structural determinations of two new structural types. The complexes $\{K(DMF)_7Ln[M(CN)_4]_2\}_\infty$ (M(II) = Ni, Ln(III) = Eu, **1**; M(II) = Pt, Ln(III) = Yb, **2**) in the solid state consist of neutral puckered sheetlike arrays, with a repeating unit like that of the type **A** and **B** arrays. Between the sheets $(DMF)_4K_2[M(CN)]_4$ units act as spacers. The second new structural type, $\{(NH_4)(DMF)_4Yb[Pt(CN)_4]_2\}_\infty$, **3**, consists of negatively charged, square, parallel columns bundled through N−H···NC hydrogen bonds between NH_4^+ ions and terminal CN from the columns.

Results and Discussion

Syntheses of $\{K(DMF)_7Eu[Ni(CN)_4]_2\}_\infty$, 1, and $\{K(DMF)_7Yb[Pt(CN)_4]_2\}_4$, 2. Complexes of the general formula {K-

(1) Earlier, related publications in this series are: (a) Knoeppel, D. W.; Shore, S. G. *Inorg. Chem.* **1996**, *35*, 1747. (b) Shore, S. G.; Deng, H.; Knoeppel, D. W.; Liu, J.; White, J. P., III; Chun, S.-H. *J. Alloys Compd.* **1997**, *249*, 25. (c) Knoeppel, D. W.; Shore, S. G. *Inorg. Chem.* **1996**, *35*, 5328. (d) Knoeppel, D. W.; Liu, J.; Meyers, E. A.; Shore, S. G. *Inorg. Chem.* **1998**, *37*, 4828. (e) Liu, J.; Meyers, E. A.; Cowan, J. A.; Shore, S. G. *Chem. Commun.* **1998**, 2043. (f) Liu, J.; Meyers, E. A.; Shore, S. G. *Inorg. Chem.* **1998**, *37*, 5410. (g) Du, B.; Meyers, E. A.; Shore, S. G. *Inorg. Chem.* **2000**, *39*, 4639. (h) Liu, J.; Knoeppel, D. W.; Liu, S.; Meyers, E. A.; Shore, S. G. *Inorg. Chem.*, in press. (i) Du, B.; Ding, E.; Meyers, E. A.; Shore, S. G. *Inorg. Chem.*, in press.

(2) See ref 1e for references to selected applications.

(3) Rath, A.; Liu, J.; Shore, S. G.; Aceves, E.; Mitome, J.; Ozkan U. S. *J. Mol. Catal. A: Chem.* **2001**, *165*, 103.

(4) (a) Du, B. Ph.D. Dissertation, The Ohio State University, 2000. (b) Du, B.; Ebels, U. S.; Wigen, P. E.; Shore S. G. Manuscript in preparation.

(5) van Vleck, J. H. *Rev. Mod. Phys.* **1953**, *25*, 220. (b) Mattis, D. C. *The Theory of Magnetism I*; Springer: Berlin, 1981.

10.1021/ic0014787 CCC: $20.00
Published on Web 07/13/2001

Table 1. Crystallographic Data for $\{K(DMF)_7Ln[M(CN)_4]_2\}_\infty$ (M = Ni, Ln = Eu, **1**; M = Pt, Ln = Yb, **2**) and $\{(NH_4)(DMF)_4Yb[Pt(CN)_4]_2\}_\infty$, **3**

	1	**2**	**3**
empirical formula	$C_{29}H_{49}N_{15}O_7KEuNi_2$	$C_{29}H_{49}N_{15}O_7KYbPt_2$	$C_{20}H_{32}N_{13}O_4YbPt_2$
formula weight, amu	1028.31	1322.15	1081.81
space group (No.)	*P§* (2)	*P§* (2)	$P2_1/c$(14)
a, Å	8.797(2)	8.852(1)	9.032(1)
b, Å	15.621(3)	15.673(1)	29.062(1)
c, Å	17.973(6)	17.946(1)	15.316(1)
α, deg	105.48(2)	105.46(1)	
β, deg	98.60(2)	99.10(1)	94.51(1)
γ, deg	98.15(2)	98.59(1)	
vol, Å^3	2310.3(9)	2321.9(3)	4008.0(5)
Z	2	2	4
D_{calcd}, g cm^{-3}	1.478	1.892	1.793
T, °C	26	−60	−60
λ, Å	Mo K_α (0.71073)	Mo K_α (0.71073)	Mo K_α (0.71073)
μ, mm^{-1}	2.291	8.155	9.315
R^a (F_o)	0.0467	0.0462	0.0819
$R_w{}^b$ (F_w)	0.1250	0.1428	0.2595

[a] $R_1 = \sum||F_o| - |F_c||/\sum|F_o|$. [b] $wR_2 = \{\sum w(F_o^2 - F_c^2)^2/\sum w(F_o^2)^2\}^{1/2}$.

$(DMF)_7Ln[M(CN)_4]_2\}_\infty$ (M = Ni, Ln = Eu, **1**; M = Pt, Ln = Yb, **2**) were prepared quantitatively through metathesis reactions between anhydrous $LnCl_3$ and $K_2[M(CN)_4]$ at a 1:2 molar ratio in dry DMF solution at ambient temperature (eq 1).

$$LnCl_3 + 2K_2[M(CN)_4] + 7DMF \rightarrow 1/\infty\{K(DMF)_7Ln[M(CN)_4]_2\}_\infty + 3KCl\downarrow \quad (1)$$

M = Ni, and Ln = Eu, **1**. M = Pt, and Ln = Yb, **2**

Formation of **1** was complete in 5 days, and the formation of **2** was complete in 7 days. To obtain the solid complexes, it was necessary to deposit them from supersaturated mother liquors. Otherwise, the previously reported[1b,d,h] type **B** one-dimensional arrays of general formula $\{(DMF)_{10}Ln_2[M(CN)_4]_3\}_\infty$ were obtained under normal conditions, because they are less soluble in DMF than the two-dimensional complexes **1** and **2**. The crystal growth processes were slow for both the one- and two-dimensional products. Supersaturated solutions from which **1** and **2** crystallized were prepared by applying dynamic vacuum. It was critical to minimize mechanical disturbances to the systems in order to avoid premature crystallization of undesired one-dimensional products. Once the first batch of the desired crystals formed, which could be easily recognized by the formation of the large shell-shaped crystals, they were used as seed crystals in the subsequent experiments. This greatly facilitated the preparation of the desired complexes, **1** and **2** and minimized the possibility of accidentaly crystallizing the type **B** one-dimensional array.

The long reaction times are in part due to the slow solvation rates of $LnCl_3$; however, the reactions were far from complete long after all solid $LnCl_3$ reactants disappeared in the reaction mixtures. In fact, the reactions did not immediately take place when pre-prepared DMF solutions of $EuCl_3$ and $K_2[Ni(CN)_4]$ were mixed together. Similarly, it was observed in the preparation of the one-dimensional complexes that premature termination of the reactions produced mixtures of mono-chloride complexes $\{(DMF)_5Sm[Ni(CN)_4]Cl\}_\infty$ and $\{(DMA)_4Yb[Ni(CN)_4]Cl\}_\infty$ among other byproducts.[1b,d] The long reaction times can be attributed to the kinetically stable solvated inner sphere coordination chloride complex ions $[(DMF)_6LnCl_2]^+$ and $[(DMF)_7LnCl]^{2+}$.[6]

(6) Ishiguro, S.-I.; Takahashi, R. *Inorg. Chem.* **1991**, *30*, 1854.

Structures of the Sheet-Like Arrays $\{K(DMF)_7Eu[Ni(CN)_4]_2\}_\infty$, 1, and $\{K(DMF)_7Yb[Pt(CN)_4]_2\}_\infty$, 2. Both complexes **1** and **2** crystallize in the triclinic space group $P\bar{1}$. They are isomorphous and isostructural. Crystallographic data for **1** and **2** are given in Table 1. Table 2 lists selected bond lengths and angles for **1** and **2**. Figures 1 and 2 depict a structure that is representative of that of complex **1** and complex **2**. This structure, Figure 1, consists of infinite layers of neutral two-dimensional, parallel, puckered sheets of formula $\{(DMF)_{10}Ln_2[M(CN)_4]_3\}_\infty$ and interstitial $(DMF)_4K_2[M(CN)_4]$ units between the sheets. The infinite sheet structure is formed from hexagonal repeating units that share common edges. These hexagons are formed from three linked $(DMF)_{10}Ln_2[M(CN)_4]_3$ units. These hexagonal rings adopt a chair conformation similar to that of a cyclohexane molecule (Figure 2). Six lanthanide atoms occupy the corners of the hexagon. Six trans-bridging $[M(CN)_4]^{2-}$ units form the edges of the hexagon. Each corner is shared by three hexagonal units; and each edge is shared by two units. The edge sharing hexagonal units form the slightly puckered two-dimensional infinite sheet (Figure 1). They are stacked on top of each other, separated by the interstitial $(DMF)_4K_2[M(CN)_4]$ units positioned approximately above and below the centers of the hexagons (Figure 2). The formula of the sheet $\{(DMF)_{10}Ln_2[M(CN)_4]_3\}_\infty$, is also the formula of the one-dimensional complexes of type **A**, a single-strand chain structure, and type **B**, a double-strand chain[1d] structure (Figure 3).

Note: In the type **A** structure, only the trans CN ligands of the $M(CN)_4$ units form M−CN−Ln bridges. In the type **B** structure, both cis and trans CN ligands, but not on the same $M(CN)_4$ unit, form M−CN−Ln bridges, while in complexes **1** and **2** only trans CN ligands form bridges. The sheets are neutral without requiring charge compensation from the components of the interstitial unit, $(DMF)_4K_2[M(CN)_4]$. However, the presence of the interstitial $(DMF)_4K_2[M(CN)_4]$ units appears to be a critical requirement for the formation of the sheet structure. The nonbridging $[M(CN)_4]^{2-}$ units are positioned along the centers of the hexagons above and below the sheets and are approximately perpendicular to the sheets, each interacting with four K^+ ions through its cyano groups. The distances between the transition metals from layer to layer are 8.798(5) and 8.85(2) Å, respectively, for Ni or Pt. The interstitial $(DMF)_4K_2[M(CN)_4]$ units act as spacers.

There is only one crystallographically independent site for Eu(III) or Yb(III) in the unit cells of **1** and **2**. However, four

Table 2. Selected Bond Lengths (Å) and Angles (Deg) for $\{K(DMF)_7Ln[M(CN)_4]_2\}_\infty$ (M = Ni, Ln = Eu, **1**; M = Pt, Ln = Yb, **2**) and $\{(NH_4)(DMF)_4Yb[Pt(CN)_4]_2\}_\infty$, **3**[a]

Bond lengths for **1**

Eu−O(1)	2.399(5)	Eu−N(3)	2.519(6)	Ni(3)−C(5)	1.860(7)	C(3)−N(3)	1.161(9)
Eu−O(2)	2.373(6)	Eu−N(5)	2.528(6)	Ni(3)−C(6)	1.879(10)	C(4)−N(4)	1.151(11)
Eu−O(3)	2.381(5)	Ni(1)−C(1)	1.873(7)	Ni(4)−C(7)	1.864(10)	C(5)−N(5)	1.150(9)
Eu−O(4)	2.392(5)	Ni(1)−C(2)	1.863(9)	Ni(4)−C(8)	1.853(11)	C(6)−N(6)	1.144(11)
Eu−O(5)	2.392(6)	Ni(2)−C(3)	1.853(7)	C(1)−N(1)	1.138(9)	C(7)−N(7)	1.141(12)
Eu−N(1)	2.529(6)	Ni(2)−C(4)	1.871(9)	C(2)−N(2)	1.145(11)	C(8)−N(8)	1.125(13)

Bond angles for **1**

O(2)−Eu−O(3)	119.8(2)	O(4)−Eu−N(1)	72.2(2)	O(2)−Eu−N(3)	141.7(2)	C(1)−N(1)−Eu	174.2(6)
O(2)−Eu−O(4)	74.0(2)	O(5)−Eu−N(1)	141.7(2)	O(3)−Eu−N(3)	76.9(2)	C(3)−N(3)−Eu	170.8(7)
O(3)−Eu−O(4)	137.29(19)	O(1)−Eu−N(1)	73.64(19)	O(4)−Eu−N(3)	72.0(2)	C(5)−N(5)−Eu	163.8(6)
O(2)−Eu−O(5)	73.9(2)	N(3)−Eu−N(5)	142.2(2)	O(5)−Eu−N(3)	81.3(2)	N(1)−C(1)−Ni(1)	178.7(7)
O(3)−Eu−O(5)	70.9(2)	N(3)−Eu−N(1)	108.0(2)	O(1)−Eu−N(3)	74.9(2)	N(2)−C(2)−Ni(1)	176.5(8)
O(4)−Eu−O(5)	76.0(2)	N(5)−Eu−N(1)	84.2(2)	O(2)−Eu−N(5)	75.2(2)	N(3)−C(3)−Ni(2)	177.6(7)
O(2)−Eu−O(1)	139.69(18)	C(2)#1−Ni(1)−C(1)	89.1(3)	O(3)−Eu−N(5)	74.6(2)	N(4)−C(4)−Ni(2)	179.6(10)
O(3)−Eu−O(1)	76.44(19)	C(2)−Ni(1)−C(1)	90.9(3)	O(4)−Eu−N(5)	144.5(2)	N(5)−C(5)−Ni(3)	178.3(7)
O(4)−Eu−O(1)	121.0(2)	C(3)#2-Ni(2)−C(4)	89.6(3)	O(5)−Eu−N(5)	111.6(2)	N(6)−C(6)−Ni(3)	177.8(8)
O(5)−Eu−O(1)	143.0(2)	C(3)−Ni(2)−C(4)	90.4(3)	O(1)−Eu−N(5)	74.7(2)	N(7)−C(7)−Ni(4)	178.2(11)
O(2)−Eu−N(1)	77.3(2)	C(5)−Ni(3)−C(6)#3	89.0(3)	C(8)−Ni(4)−C(7)	89.9(4)	N(8)−C(8)−Ni(4)	179.3(12)
O(3)−Eu−N(1)	147.0(2)	C(5)−Ni(3)−C(6)	91.0(3)	C(8)#4−Ni(4)−C(7)	90.1(4)		

Bond lengths for **2**

Yb−O(1)	2.340(12)	Yb−N(3)	2.391(15)	Pt(3)−C(5)	2.00(2)	C(3)−N(3)	1.15(2)
Yb−O(2)	2.322(11)	Yb−N(5)	2.417(16)	Pt(3)−C(6)	2.00(2)	C(4)−N(4)	1.17(2)
Yb−O(3)	2.298(11)	Pt(1)−C(1)	1.965(18)	Pt(4)−C(7)	2.02(2)	C(5)−N(5)	1.14(2)
Yb−O(4)	2.305(12)	Pt(1)−C(2)	2.00(2)	Pt(4)−C(8)	1.98(2)	C(6)−N(6)	1.18(3)
Yb−O(5)	2.305(12)	Pt(2)−C(3)	2.01(2)	C(1)−N(1)	1.14(2)	C(7)−N(7)	1.13(2)
Yb−N(1)	2.445(14)	Pt(2)−C(4)	1.97(2)	C(2)−N(2)	1.14(2)	C(8)−N(8)	1.13(2)

Bond angles for **2**

C(1)−Pt(1)−C(2)	88.2(8)	O(5)−Yb−O(2)	142.4(4)	O(5)−Yb−N(5)	82.1(5)	N(1)−C(1)−Pt(1)	177.4(16)
C(1)−Pt(1)−C(2)#1	91.8(8)	O(4)−Yb−O(2)	76.7(4)	O(4)−Yb−N(5)	77.7(5)	N(2)−C(2)−Pt(1)	179(2)
C(4)−Pt(2)−C(3)	91.1(7)	O(3)−Yb−O(1)	73.6(4)	O(2)−Yb−N(5)	73.2(5)	N(3)−C(3)−Pt(2)	175.8(15)
C(4)#2−Pt(2)−C(3)	88.9(7)	O(5)−Yb−O(1)	75.0(5)	O(1)−Yb−N(5)	72.9(5)	N(4)−C(4)−Pt(2)	177.1(18)
C(5)−Pt(3)−C(6)	89.7(7)	O(4)−Yb−O(1)	137.1(4)	O(3)−Yb−N(1)	77.5(4)	N(5)−C(5)−Pt(3)	176.9(18)
C(5)#3−Pt(3)−C(6)	90.3(7)	O(2)−Yb−O(1)	121.7(4)	O(5)−Yb−N(1)	141.5(5)	N(6)−C(6)−Pt(3)	177.1(19)
C(8)−Pt(4)−C(7)	88.6(8)	O(3)−Yb−N(3)	74.2(4)	O(4)−Yb−N(1)	147.6(5)	N(7)−C(7)−Pt(4)	178.9(19)
C(8)#4−Pt(4)−C(7)	91.4(8)	O(5)−Yb−N(3)	111.3(5)	O(2)−Yb−N(1)	74.1(4)	N(8)−C(8)−Pt(4)	179(2)
O(3)−Yb−O(5)	74.4(4)	O(4)−Yb−N(3)	74.3(5)	O(1)−Yb−N(1)	72.0(4)	C(1)−N(1)−Yb	173.3(14)
O(3)−Yb−O(4)	119.1(4)	O(2)−Yb−N(3)	76.0(5)	N(3)−Yb−N(1)	85.4(5)	C(3)−N(3)−Yb	165.9(14)
O(5)−Yb−O(4)	70.6(5)	O(1)−Yb−N(3)	143.9(5)	N(5)−Yb−N(1)	106.4(5)	C(5)−N(5)−Yb	172.1(16)
O(3)−Yb−O(2)	140.0(4)	O(3)−Yb−N(5)	142.9(5)	N(3)−Yb−N(5)	142.1(5)		

Bond lengths for **3**

Pt(1)−C(1)	1.94(3)	Yb−O(45)	2.36(4)	C(3)−N(3)	1.21(4)	C(6)−N(6)	1.09(4)
Pt(1)−C(2)	1.93(3)	Yb−N(1)#1	2.45(3)	Pt(2)−C(5)	1.94(3)	C(7)−N(7)	1.14(4)
Pt(1)−C(4)	1.94(3)	Yb−N(4)	2.36(3)	Pt(2)−C(6)	2.05(4)	C(8)−N(8)	1.16(4)
Pt(1)−C(3)	1.94(3)	Yb−N(5)#2	2.46(4)	Pt(2)−C(7)	1.95(3)	N−N(2)#6	2.97(4)
Yb−O(10)	2.32(2)	Yb−N(6)	2.39(2)	Pt(2)−C(8)	2.00(4)	N−N(3)#5	2.84(3)
Yb−O(20)	2.30(2)	C(1)−N(1)	1.17(3)	C(4)−N(4)	1.26(4)	N−N(7)	2.88(4)
Yb−O(30)	2.35(3)	C(2)−N(2)	1.17(4)	C(5)−N(5)	1.14(4)	N−N(8)#4	2.84(4)
Yb−O(40)	2.33(3)						

Bond angles for **3**

C(2)−Pt(1)−C(4)	177.8(12)	O(20)−Yb−N(6)	143.4(10)	N(6)−Yb−N(5)#2	80.2(10)	N(4)−C(4)−Pt(1)	174(3)
C(2)−Pt(1)−C(3)	90.9(12)	O(10)−Yb−N(6)	107.1(9)	N(1)#1−Yb−N(5)#2	76.3(10)	N(5)−C(5)−Pt(2)	170(3)
C(4)−Pt(1)−C(3)	90.4(12)	O(40)−Yb−N(6)	77.3(12)	O(20)−Yb−O(10)	83.5(9)	N(6)−C(6)−Pt(2)	178(3)
C(2)−Pt(1)−C(1)	88.5(11)	O(30)−Yb−N(6)	70.7(9)	O(20)−Yb−O(40)	120.3(15)	N(7)−C(7)−Pt(2)	175(3)
C(4)−Pt(1)−C(1)	90.1(11)	O(45)−Yb−N(6)	88.8(14)	O(10)−Yb−O(40)	134.7(14)	C(7)−N(7)−N(4H)	170(3)
C(3)−Pt(1)−C(1)	178.7(12)	O(20)−Yb−N(1)#1	74.7(9)	O(20)−Yb−O(30)	144.2(10)	N(8)−C(8)−Pt(2)	178(4)
C(5)−Pt(2)−C(7)	177.0(13)	O(10)−Yb−N(1)#1	73.2(8)	O(10)−Yb−O(30)	72.2(10)	C(1)−N(1)−Yb#3	162(2)
C(5)−Pt(2)−C(8)	88.9(11)	O(40)−Yb−N(1)#1	146.0(11)	O(40)−Yb−O(30)	67.0(16)	C(4)−N(4)−Yb	157(3)
C(7)−Pt(2)−C(8)	89.6(13)	O(30)−Yb−N(1)#1	120.4(9)	O(20)−Yb−O(45)	97.3(15)	C(5)−N(5)−Yb#2	165(3)
C(5)−Pt(2)−C(6)	91.6(10)	O(45)−Yb−N(1)#1	133.9(14)	O(10)−Yb−O(45)	152.3(14)	C(6)−N(6)−Yb	163(3)
C(7)−Pt(2)−C(6)	89.7(12)	O(20)−Yb−N(5)#2	72.8(9)	O(40)−Yb−O(45)	26.1(15)	N(8)#4−N−N(3)#5	104.0(11)
C(8)−Pt(2)−C(6)	177.3(15)	O(10)−Yb−N(5)#2	145.3(9)	O(30)−Yb−O(45)	92.8(16)	N(8)#4−N−N(7)	118.4(11)
N(4)−Yb−N(5)#2	119.9(12)	O(40)−Yb−N(5)#2	79.8(14)	O(20)−Yb−N(4)	74.4(12)	N(3)#5−N−N(7)	105.9(11)
N(4)−Yb−N(6)	141.8(11)	O(30)−Yb−N(5)#2	139.5(9)	O(10)−Yb−N(4)	75.4(9)	N(8)#4−N−N(2)#6	112.7(11)
N(4)−Yb−N(1)#1	137.9(9)	O(45)−Yb−N(5)#2	58.3(15)	O(40)−Yb−N(4)	75.4(11)	N(3)#5−N−N(2)#6	104.1(10)
N(6)−Yb−N(1)#	175.2(9)	N(1)−C(1)−Pt(1)	178(3)	O(30)−Yb−N(4)	74.3(11)	N(7)−N−N(2)#6	110.2(12)
N(4)−Yb−O(45)	78.1(13)	N(2)−C(2)−Pt(1)	179(3)	N(3)−C(3)−Pt(1)	177(3)		

[a] Symmetry transformations used to generate equivalent atoms of: (a) **1**: #1 $-x, -y+2, -z$; #2 $-x, -y+2, -z+1$; #3 $-x, -y+1, -z$; #4 $-x+1, -y+1, -z+1$. (b) **2**: #1 $-x+1, -y, -z+1$; #2 $-x+1, -y-1, -z+1$; #3 $-x+1, -y, -z+2$; #4 $-x+2, -y+1, -z+2$. and (c) **3**: #1 $x-1, y, z$; #2 $-x-1, -y+1, -z+2$; #3 $x+1, y, z$; #4 $x, -y+1/2, z-1/2$; #5 $-x-1, -y+1, -z+1$; #6 $-x, -y+1, -z+1$.

independent sites, all at crystallographically special positions, were found for transition metals Ni(II) and Pt(II). Three of them are parts of the hexagonal units, and a fourth one belongs to the interstitial $(DMF)_4K_2[M(CN)_4]$ fragment. The hexagonal

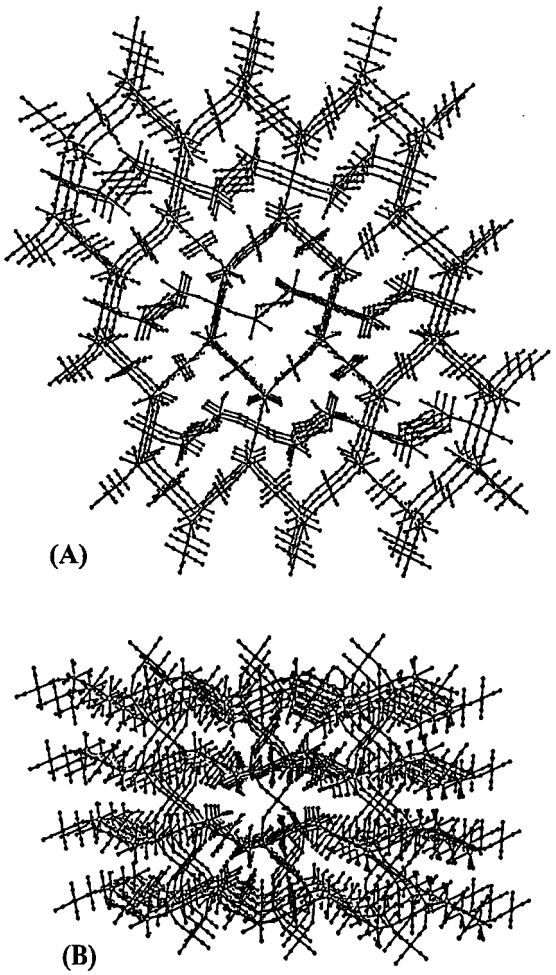

Figure 1. Views of the extended sheet structure of the isomorphous and isostructural complexes $\{K(DMF)_7Ln[M(CN)_4]_2\}_\infty$ (Ln = Eu, M = Ni, **1**; Ln = Yb, M = Pt, **2**). (A) Projection down the *a* axis. (B) Projection down the *c* axis.

repeating unit was generated through symmetry transformations. The coordination geometries of the lanthanides are bicapped trigonal prismatic while the coordination geometries of the transition metals are square planar.

The Eu−O bond distances in **1** range from 2.373(6) to 2.399(5) Å with an average of 2.387(5) Å (Table 2). The Eu−N bond distances vary from 2.519(6) to 2.529(6) Å with an average of 2.525(6) Å. The average of the Eu−O bond distance is slightly longer than those found for the eight-coordinated complexes $\{(DMF)_{10}Eu_2[M(CN)_4]_3\}_\infty$ (M = Ni, Pd),[1b,d,h] but are significantly shorter than those reported for $(H_2O)_{12}Eu_2[Pd(CN)_4]_3$, a nine-coordinated complex.[7] (The average of the Eu−N bond distances is in good agreement with most of the related eight-coordinated complexes. In comparison, $K(H_2O)_2Eu[Ru(CN)_6]$-$A2H_2O$, also an eight-coordinated complex, displays unusually long Eu−O(H_2O) bond distances presumably because of the steric effect imposed by its six bulky [$Ru(CN)_6$] groups.[8]

The Yb−O bond distances in **2** range from 2.30(1) to 2.34(1) Å (Table 2). The Yb−N bond distances range from 2.39(2) to 2.45(1) Å. They are in good agreement with those reported for $\{(DMF)_{10}Yb_2[M(CN)_4]_3\}_\infty$ (M = Ni, Pd, Pt),[1a,d,h] and are comparable with those found in $CsYb(EDTA)(H_2O)_2$, also an eight-coordinated complex.[9] The Yb−O and Yb−N bonds in **2** are shorter than the Eu−O and Eu−N bonds in **1** because of the "lanthanide contraction".[10] The difference in the average

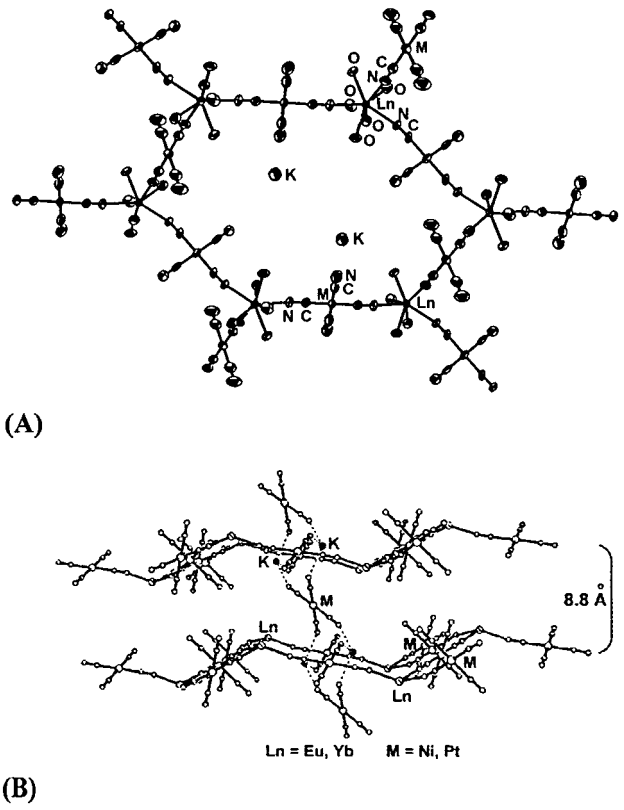

Figure 2. (A) View of the repeating hexagonal unit of the extended sheet structure of $\{K(DMF)_7Ln[M(CN)_4]_2\}_\infty$ (Ln = Eu, M = Ni, **1**; Ln = Yb, M = Pt, **2**). Only oxygens of DMF atoms coordinated to Ln are shown. (B) View of the placement of interstitial $K_2[M(CN)_4]$ units between the hexagonal repeating units of **1** and **2**.

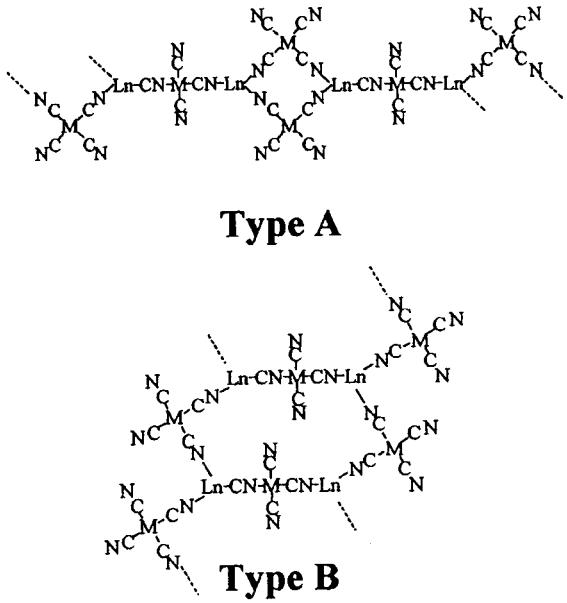

Figure 3. Type **A** and type **B** single- and double-strand chains formed from the repeating unit $\{[M(CN)_4](DMF)_5Ln[M(CN)_4]Ln(DMF)_5[M(CN)_4]\}$.

(7) Klement, U. *Z. Kristallogr.* **1993**, *208*, 285, 288. Bond distances and angles were calculated based on the crystallographic information and atomic coordinates provided by the author.
(8) Mullica, D. F.; Sappenfield, E. L. *Inorg. Chim. Acta* **1997**, *258*, 101.
(9) Nassimbeni, L. R.; Wright, M. R. W.; van Niekerk, J. C.; McCallum, P. A. *Acta Crystallogr. B* **1979**, *35*, 1341.
(10) Huheey, J. E. *Inorganic Chemistry*, 3rd ed.; Harper & Row: New York, 1983.

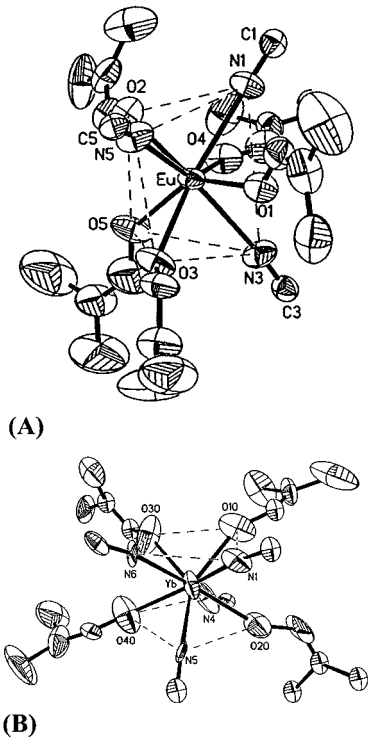

Figure 4. (A) Coordination geometry of Eu in complex **1**. (B) Coordination geometry of Yb in complex **3**.

bond distances is 0.073 Å between Eu−O in **1** and Yb−O in **2**. The difference is 0.107 Å between Eu−N in **1** and Yb−N in **2**. The projected difference of the radii is 0.081 Å between eight-coordinated Eu^{3+} and Yb^{3+} ions based upon the Shannon radii.[11]

In complexes **1** and **2**, the Ln(III) (Ln = Eu, Yb) centers are eight-coordinated to the three nitrogen atoms from the bridging CN^- ligands and the five oxygen atoms from the coordinated DMF molecules. The coordination geometry around the Ln(III) centers can be best described as a distorted bicapped trigonal prism (Figure 4A), which is the least common of the three coordination geometries (dodecahedron, square antiprism, and bicapped trigonal prism) for an eight-coordinated lanthanide complex.[12] This differs from the square antiprismatic geometry observed for the one-dimensional complexes $\{(DMF)_{10}Ln_2[M(CN)_4]_3\}_\infty$.[1b,d,h] The assignment of the coordination geometry follows the method described in our previous paper,[1g] which is based primarily on the criteria proposed by Porai−Koshits and Aslanov[13a] (see the Supporting Information). Classic sphere-inscribed models, of Hoard and Silverton,[14a] are difficult to apply because of distortion resulting from the different ligand−metal bond lengths, which are inherent for complexes with mixed ligating groups.[14]

The coordination geometries around the Ni and Pt atoms are slightly distorted square planes, with small distortions of the C−M−C angles from 90°. The three bridging $[M(CN)_4]^{2-}$ units around the Ln(III) centers are arranged in a propeller-like configuration. The dihedral angles between the $[Pt(CN)_4]^{2-}$ units in **2**, for example, are 77.9(7)° (Pt1/Pt2), 77.7(6)° (Pt2/Pt3), and 76.4(6)° (Pt1/Pt3). All of the bond distances and angles appear to be normal as compared to other related complexes.[1a,d,15−17]

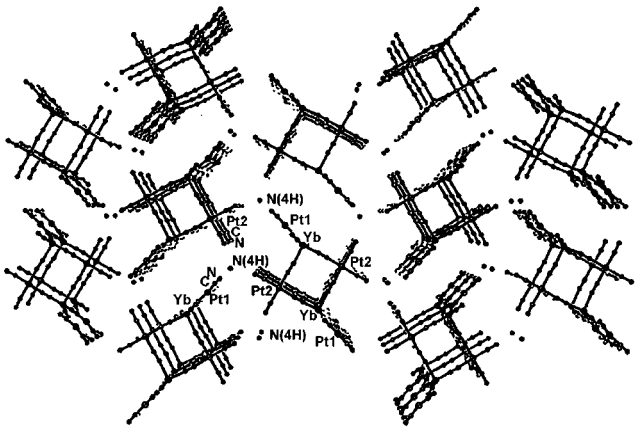

Figure 5. Extended three-dimensional, column-like structure of $\{(NH_4)(DMF)_4Yb[Pt(CN)_4]_2\}_\infty$, **3**; projection down the *a* axis.

Synthesis of Complex $\{(NH_4)(DMF)_4Yb[Pt(CN)_4]_2\}_\infty$, 3. Complex **3** was obtained in high yield (∼86%) from the metathesis reaction between anhydrous $YbCl_3$ and $(NH_4)_2[Pt(CN)_4]$ at 1:2 molar ratio in DMF solution at ambient temperature over a period of 7 days (eq 2).

$$YbCl_3 + 2(NH_4)_2[Pt(CN)_4] + 4\ DMF \rightarrow 1/\infty\{(NH_4)(DMF)_4Yb[Pt(CN)_4]_2\}_\infty + 3NH_4Cl\downarrow \quad (2)$$

This reaction is similar to the one for the preparation of complex **2** (eq 1), in which the potassium salt of tetracyanoplatinate is employed. However, complexes **2** and **3** are structurally so different that they must follow different assembly pathways. The difference is undoubtedly due to the ability of the NH_4^+ ion to form hydrogen bonds with the nitrogens of cyano groups of the $[Pt(CN)_4]^{2-}$ units in **3**.

Structure of the Complex $\{(NH_4)(DMF)_4Yb[Pt(CN)_4]_2\}_\infty$, 3. Complex **3** crystallizes in the monoclinic space group $P2_1/c$. Crystallographic data for **3** are listed in Table 1. Table 2 contains selected bond lengths and angles. X-ray single-crystal analysis of **3**, Figure 5, reveals an array that consists of negatively charged square, parallel columns that are charge compensated by NH_4^+ ions. The NH_4^+ ions serve as links between the columns through N−H···NC hydrogen bridges. Each NH_4^+ ion is bound to three columns. The negative charge of the columns is compensated by the interstitial NH_4^+ ions between the columns. Figure 5 is a projection down the *a* axis, a view that depicts the tops of the columns and reveals three columns clustered around the nitrogens of NH_4^+ ions. Figure 6 is a projection down the *c* axis. It reveals the individual columns.

Each column is composed of Yb_2Pt_2 squares that are stacked on top of each other. Normal to each square are two $Pt(CN)_4$ units above the plane and below that are bound to the Yb atoms. They serve as NC−Pt−CN bridges between that square and the one above and the one below. The remaining two CN units

(11) Shannon, R. D. *Acta Crystallogr. A* **1976**, *32*, 751.
(12) (a) Lippard, S. J. In *Progress in Inorganic Chemistry*; Cotton, F. A., Ed.; Interscience: New York, 1967; Vol. 8, p 109. (b) Sinha, S. P. *Struct. Bonding* **1976**, *25*, 69.
(13) (a) Porai-Koshits, M. A.; Aslanov, L. A. *Zh. Strukt. Khim.* **1972**, *13*, 266. (b) Lippard, S. J.; Russ, B. J. *Inorg. Chem.* **1968**, *7*, 1686.
(14) (a) Hoard, J. L.; Silverton, J. V. *Inorg. Chem.* **1963**, *2*, 235. (b) Muetterties, E. L.; Wright, C. M. *Quart. Rev.* **1967**, *21*, 109. (c) Muetterties, E. L. *Inorg. Chem.* **1973**, *12*, 1963. (d) Kepert, D. L. In *Progress in Inorganic Chemistry*; Lippard, S. J., Ed.; Interscience: New York, 1978; Vol. 24, p 179. (e) Kepert, D. L. *J. Chem. Soc.* **1965**, 4736.
(15) Bailey, W. E.; Williams, R. J.; Milligan, W. O. *Acta Crystallogr. B* **1973**, *29*, 1365.
(16) (a) Holzapfel, W.; Yersin, H.; Gliemann, G. *Z. Kristallogr.* **1981**, *157*, 47. (b) Gliemann, G.; Yersin, H. *Struct. Bonding* **1985**, *62*, 87.
(17) (a) Moreau-Colin, M. L. *Struct. Bonding* **1972**, *10*, 167. (b) Cernak, J.; Dunaj-Jurco, M.; Melnik, M.; Chomic, J.; Skorsepa, J. *Rev. Inorg. Chem.* **1988**, *9*, 259.

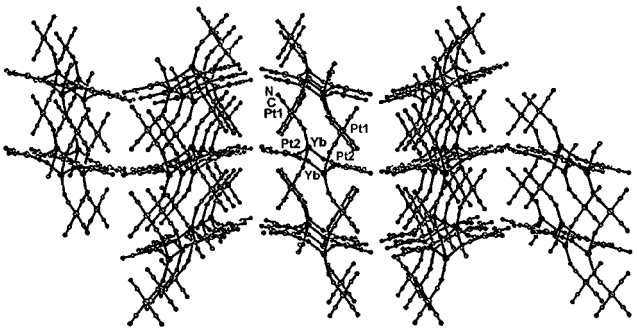

Figure 6. Extended three-dimensional, column-like structure of $\{(NH_4)(DMF)_4Yb[Pt(CN)_4]_2\}_\infty$, **3**; projection down the *c* axis. NH_4^+ omitted for clarity.

on the bridging $Pt(CN)_4$ units are connected to the NH_4^+ ion through hydrogen bridges. For the sake of clarity, the NH_4^+ ions are not shown in Figure 6.

Figure 7 is a schematic representation that reveals details of a three column cluster that surround NH_4^+ ions. Each column is identical. However, columns labeled **I** and **II** are bound to NH_4^+ ions in a manner different from that in column **III**. There is only one crystallographically independent site for Yb atoms, but there are two for Pt atoms. The $Pt(CN)_4$ units of Pt1 link the stacked Yb_2Pt_2 squares to form the columns while the other $Pt(CN)_4$ units of Pt2 form corners of theYb_2Pt_2 squares through coordination of CN units with the Yb corners of the square. The remaining CN units on Pt2 form hydrogen bonds with NH_4^+ ions.

The structure of **3** can be viewed in terms of the "ladder-like", double-strand type B structure found in one-dimensional complexes (Figure 3). By replacing the single trans-bridging $[Pt(CN)_4]^{2-}$ units with double cis-bridging $[Pt(CN)_4]^{2-}$ units between the two $-Pt-CN-Pt-$ zigzag chains,[1d] the column structure of **3** is generated, Figure 8. The double cis-bridging $[Pt(CN)_4]^{2-}$ units produce square Yb_2Pt_2 fragments resembling the Ln_2Ni_2 fragments found in the type **A** structure (Figure 3). In essence, the column structure can be viewed as a hybrid of the type **A** and type **B** structures.

The Yb−O bond distances range from 2.30(2) to 2.36(4) Å, and the Yb−N bond distances vary from 2.36(3) to 2.46(4) Å. They are in good agreement with those reported for $\{(DMF)_{10}Yb_2[M(CN)_4]_3\}_\infty$ (M = Ni, Pd, Pt),[1a,d,h] CsYb(EDTA)$(H_2O)_2$,[9] and complex **2**, all of them eight-coordinated complexes.

To our knowledge, complex **3** is the only known example in which there are four bridging $[M(CN)_4]^{2-}$ units coordinated to a Ln(III) center. The coordination geometry is perhaps best represented as a severely distorted square antiprismatic geometry, Figure 4B. Angular criteria (see the Supporting Information) suggest a coordination geometry between an ideal square antiprism and a bicapped trigonal prism. The upper face of the square antiprism, defined by O20−N4−O40−N5, has a root-mean-square deviation of 0.028 Å from planarity while the lower face, defined by O10−N1−N6−O30, has a root-mean-square deviation of 0.10 Å from planarity. The least squares planes of the two squares are almost parallel to each other. The dihedral angle is 5(2)°. Each plane consists of two N atoms from the bridging $[Pt(CN)_4]^{2-}$ units and two O atoms from DMF molecules.

Three of the four DMF molecules coordinated to the Yb atom are disordered; the fourth one has well defined positional parameters. Each of the three disordered DMF molecules were resolved into and anistropically refined as two DMF molecules

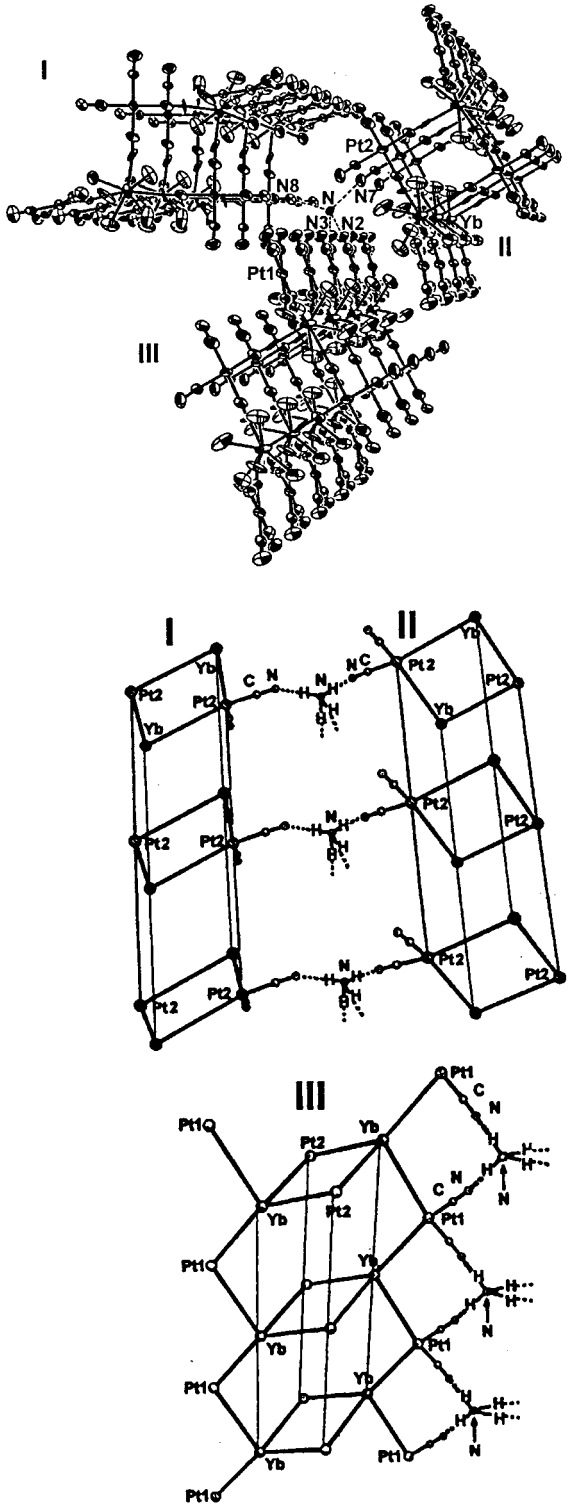

Figure 7. View of three columns hydrogen bonded to NH_4^+ ions and schematic representation of NH_4^+ linking the columns through hydrogen bonding with CN and the formation of the columns through vertical linking of Pt_2Yb_2 cores by $Pt(CN)_4$ units. Note: Thin, parallel, vertical lines only delineate columns. They are not bonds.

with their site occupancies adding up to unity. The site occupancies for each DMF pair are 0.39/0.61, 0.32/0.67, and 0.48/0.52 for DMF molecules corresponding to O20, O30, and O40, respectively. This kind of disorder is commonly observed among one-dimensional complexes.[1d] However, the disorder appears to be crystal lattice disorder rather than the previously suggested rotational disorder.

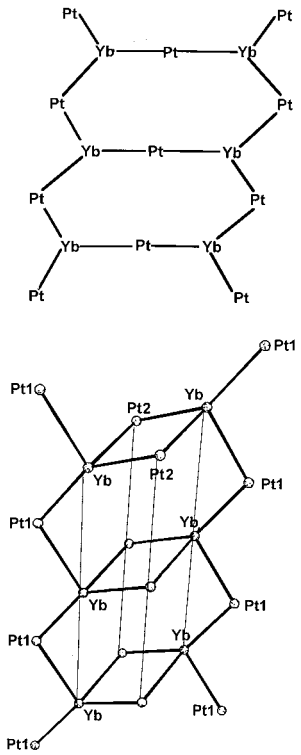

Figure 8. The relation ship between the double strand chain of the type **B** structure and the column- like arrangement in complex **3**. Note: Thin, parallel, vertical lines only delineate columns. They are not bonds.

Like **2**, the coordination geometry around Pt(II) in **3** is also a slightly distorted square plane. The Pt atoms are positioned within the least-squares planes defined by the cyanide groups. The C−Pt−C bond angles range from 89(1)° to 92(1)°. All bond distances and angles appear to be normal as compared to the other related complexes.[1a,d,15−17]

Infrared Spectra of 1, 2, and 3 and N−H···NC Hydrogen Bonds in Complex 3. Spectroscopic data and their assignments are given in the Experimental Section. Assignments are based on the structures of **1**, **2**, and **3** and related complexes previously reported.[1,15,19−22] Figures showing the CN stretching regions of the infrared spectra in Nujol mull of complexes **1**, **2**, and **3** and the KBr pellet FT-IR spectrum of complex **3** are provided in the Supporting Information.

The Nujol mull FT-IR spectrum in the CN stretching region of **1** consists of two broad bands. A band at 2122 cm^{-1} is assigned to terminal CN ligands and is in agreement with the CN stretch of $K_2[Ni(CN)_4]$. Shoulders off of this main peak at 2131 and 2106 cm^{-1} are attributed to terminal CN ligands of the trans-bridging $[Ni(CN)_4]^{-2}$ units in the $\{(DMF)_{10}Eu_2[NiCN)_4]_3\}_\infty$ sheet. Overlapping strong bands centered at 2159, 2153, and a shoulder at 2144 cm^{-1} are assigned to the bridge CN stretch. Similar observations were reported for the bridging CN ligands in related systems.[1d,20d] The CN stretching band is expected to shift to higher wavenumber when a CN ligand bridges a second metal, since stretching the CN bond results in compression of the NM bond in the isocyanide linkage[21] with a subsequent increase in the force constant of the CN bond.

Table 3. $N^+−H···N$ Type of Hydrogen Bonds: The N···N Distances (Å) and the N···N···N Angles (Deg) in Complex $\{(NH_4)(DMF)_4Yb[Pt(CN)_4]_2\}_\infty$, **3**[a]

NH_4^+−N2	2.97(4)	NH_4^+−N3	2.84(3)
NH_4^+−N7	2.88(4)	NH_4^+−N8	2.84(4)
N8−NH_4^+−N3	104(1)	N8−NH_4^+−N7	118(1)
N3−NH_4^+−N7	106(1)	N8−NH_4^+−N2	113(1)
N3−NH_4^+−N2	104(1)	N7−NH_4^+−N2	110(1)

[a] Symmetry transformations used to generate the equivalent atoms: $-x, -y+1, -z+1$ for N2; $-x-1, -y+1, -z+1$ for N3; and $x, -y+2, z-2$ for N8.

The Nujol mull FT-IR spectrum of **2** displays a main band at 2134 cm^{-1} that is assigned to the terminal CN in $[Pt(CN)_4]^{2-}$, in accord with the IR spectrum of $K_2[Pt(CN)_4]$. Shoulders at 2139 and 2129 cm^{-1} are assigned to the terminal CN ligands in the trans-bridging $[Pt(CN)_4]^{2-}$ units in the $\{(DMF)_{10}Yb_2[Pt(CN)_4]_3\}_\infty$ sheet. Two other bands in the CN stretching region at 2166 and 2184 cm^{-1} are assigned to the bridging CN ligands. The band at 2166 cm^{-1} appears to be the result of two overlapping bands.

The Nujol mull FT-IR spectrum of **3** in the CN stretch region consists of two bands, one at 2136 cm^{-1} that is assigned to terminal CN in the $[Pt(CN)_4]^{2-}$ units and one at 2152 cm^{-1} that is assigned to bridging CN ligands.

Hydrogen bonds between the interstitial NH_4^+ ions and the nitrogen atoms of the terminal CN ligands on the columns link the ammonium cation to the negatively charged columns (Figures 5 and 7). Each NH_4^+ ion is hydrogen-bonded to four terminal cyano groups from three columns. The orientations of these cyano groups toward the NH_4^+ ions are effective for hydrogen bond interaction. Figure 7 shows the arrangement of four nitrogn atoms (N2, N3, N7, N8) from terminal CN ligands around the nitrogen of NH_4^+. Five of the six CN···N···NC angles are ≤5° from the ideal angle of 109° expected for the H−N−H bond angles for an NH_4^+ ion with tetrahedral geometry (Table 3). For a typical N−H···N type of hydrogen bond, the average interatomic distance N···N is reported to be at 3.1 Å.[21] The average N···N distance in **3** is 2.88(4) Å between the NH_4^+ ions and the nitrogen atoms of the cyano groups, below the observed average N···N distance as well as the calculated N···N van der Waals contact distance (3.0 Å).[18] Attempts to refine the NH_4^+ hydrogen positions were fruitless even though their locations were resolved in the difference map. The N−H bond distances fall in the range of 0.8−1.0 Å based on the difference map.

The IR spectrum (KBr pellet) of **3** shows broad, medium strong absorption bands at 3190 cm^{-1} and 3039 cm^{-1}, corresponding to the N−H stretching vibrations.[22] A medium absorption band at 1496 cm^{-1} is assigned the N−H bending mode and is consistent with hydrogen bonding producing an increase in the bending mode frequency.[22] The bending mode for free NH_4^+ (1400 cm^{-1}) was not observed. The C−N stretching region of this spectrum displays a similar absorption pattern as observed in the Nujol IR spectrum, but with higher

(18) Hamilton, W. C.; Ibers, J. A. In *Hydrogen Bonding in Solids*; W. A. Benjamin, Inc.: New York, 1968; p 16. The observed values were determined by diffraction methods.
(19) (a) Cotton, F. A. *Chemical Applications of Group Theory*, 3rd ed.; Wiley: New York, 1990. (b) Wilson, E. B., Jr.; Decius, J. C.; Cross, P. C. In *Molecular Vibrations: The Theory of Infrared and Raman Vibrational Spectra*; McGraw-Hill Book: New York, 1955.
(20) (a) Kubas, G. J.; Jones, L. H. *Inorg. Chem.* **1974**, *13*, 2816. (b) Gans, P.; Gill, J. B.; Johnson, L. H. *J. Chem. Soc., Dalton Trans.* **1993**, 345. (c) Jerome-Lerutte, S. *Struct. Bonding* **1972**, *10*, 153. (d) Nakamoto, K. *Infrared and Raman Spectra of Inorganic and Coordination Compounds*, 4th ed.; John Wiley & Sons: New York, 1986; p 278.
(21) (a) Swanson, B. I.; Rafalko, J. J. *Inorg. Chem.* **1976**, *15*, 249. (b) Swanson, B. I. *Inorg. Chem.* **1976**, *15*, 253.
(22) Sorrell, T. N. *Interpreting Spectra of Organic Molecules*; University Science Books; Mill Valley, CA, 1988; p 33.

resolution that reveals additional shoulder bands at 2167, 2175, and 2184 cm^{-1}.[1,15,20]

Experimental Section

General Data. All manipulations were carried out on a standard high vacuum line or in a drybox under an atmosphere of dry, 99.99% pure N_2. Molecular sieves (4 Å, Linde) were heated to 150 °C under dynamic high vacuum ($10^{-4}-10^{-5}$ mmHg) overnight prior to use. DMF (Baker) was stirred over pretreated 4 Å molecular sieves for one week in a Pyrex flask. The DMF was then degassed under vacuum and then distilled at 70−80 °C into a Pyrex flask kept at −78 °C employing an 2-propanol−dry ice bath. The DMF was stored in drybox for future use. $K_2[Ni(CN)_4]\cdot H_2O$ (Strem) was dried under dynamic vacuum at 150 °C for 16 h and stored in drybox. KBr (Aldrich) was dried at 150 °C for 24 h and stored in a drybox.

Fourier transform infrared (FT-IR) spectra were recorded on a Mattson Polaris Fourier transform spectrometer with 2 cm^{-1} resolution. Nujol mull samples were prepared by grinding ca. 5 mg of the samples with a drop of mineral oil in an agate mortar and analyzed as thin films placed between KBr plates in a airtight sample holder. KBr pellets were prepared by first grinding 5 mg of the samples and ca. 95 mg of dry KBr together in an agate mortar and then compressing them into thin pellets in a metal cell. Elemental analysis was performed by Galbraith Laboratories, Inc. (Knoxville, TN).

Synthesis of Complex $\{K(DMF)_7Eu[Ni(CN)_4]_2\}_\infty$, 1, and $\{K(DMF)_7Yb[Pt(CN)_4]_2\}_\infty$, 2. Complexes **1** and **2** are isomorphous and isostructural. Since they are prepared in virtually identical procedures, a description of a general synthesis is given. In a drybox, 51.7 mg (0.2 mmol) of anhydrous $EuCl_3$ and 96.4 mg (0.4 mmol) of anhydrous $K_2[Ni(CN)_4]$ were added to a 50 mL pear-shaped flask with a magnetic stirring bar for the preparation of **1**. For the preparation of **2**, 55.9 mg (0.2 mmol) of anhydrous $YbCl_3$ and 151 mg (0.4 mmol) of anhydrous $K_2[Pt(CN)_4]$ were employed. After addition of 10 mL of dry DMF, the flask was sealed using an adaptor equipped with a Kontes Teflon stopcock. The orange mixture was stirred for 5 days at room temperature for complex **1** and 7 days for complex **2**. The reactants gradually dissolved into DMF within the first day of the reaction. During the course of the reaction, KCl precipitated as white fine particles. After removal of KCl with a vacuum line extractor, the orange solution was degassed. Then the volume of the solution was reduced to about 0.5 mL under dynamic vacuum using a high vacuum line. Extreme care was given to prevent any mechanical disturbances during this process in order to avoid the premature formation of the undesired quasi-one-dimensional product. The orange colored viscous supersaturated solution was allowed to stand for several days and produced X-ray quality orange colored single crystals of the desired complex $\{K(DMF)_7Eu[Ni(CN)_4]_2\}_\infty$, **1**, or $\{K(DMF)_7Yb[Pt(CN)_4]_2\}_\infty$, **2**. Crystals of complex **1** and of **2** formed in the shape of seashells. Yield of complex **1**: 197 mg (95.8%; calcd 205.66 mg). Anal. Calcd for $C_{29}H_{49}N_{15}O_7KEuNi_2$, **1**: C, 33.87; H, 4.80; N, 20.44. Found: C, 33.78; H, 4.73; N, 19.29. IR (Nujol mull, ν_{CN}, cm^{-1}): 2159 (s, sh), 2153 (s), 2144 (s, sh), 2131 (m, sh), 2122 (vs), 2106 (m, sh). Yield of complex **2**: 259 mg (97.9%; calcd 264.43 mg). Anal. Calcd for $C_{29}H_{49}N_{15}O_7KYbPt_2$, **2**: C, 26.34; H, 3.74; N, 15.89. Found: C, 26.99; H, 3.44; N, 15.53. IR (Nujol mull, ν_{CN}, cm^{-1}): 2184 (m), 2166 (ms), 2139 (s, sh), 2134 (vs), 2129 (s, sh).

Synthesis of Complex $\{(NH_4)(DMF)_4Yb[Pt(CN)_4]_2\}_\infty$, 3. In a drybox, 27.9 mg (0.1 mmol) of anhydrous $YbCl_3$ and 67 mg (0.2 mmol) of pre-prepared $(NH_4)_2[Pt(CN)_4]$ were added to a 25 mL pear-shaped flask with a magnetic stirring bar. After addition of 10 mL of dry DMF, the flask was sealed using a adaptor equipped with a Kontes Teflon stopcock. The mixture was stirred for 7 days at room temperature. The reactants gradually dissolved into DMF within the first day of the reaction and gave a slightly pink colored solution. During the course of the reaction, NH_4Cl precipitated out slowly as white fine particles and the solution gradually turned yellow in color. After removal of NH_4Cl with a vacuum line extractor, the yellow solution was degassed. Then the volume of the solution was reduced to about 0.5 mL under static vacuum using a high vacuum line. The viscous supersaturated solution was allowed to stand for several days. X-ray quality colorless thin plate single crystals of complex $\{(NH_4)(DMF)_4Yb[Pt(CN)_4]_2\}_\infty$, **3** were obtained. Yield: 93 mg (86%; calcd 108.18 mg). Anal. Calcd for $C_{20}H_{32}N_{13}O_4YbPt_2$, **3**: C, 22.20; H, 2.98; N, 16.84. Found: C, 21.52; H, 2.67; N, 16.00. IR (KBr, cm^{-1}): 3093 (m, br, ν_{N-H}), 3039 (m, br, ν_{N-H}), 2918 (m, sharp, ν_{C-H}), 2849 (m, sharp, ν_{C-H}), 2515 (w, br), 2362 (w, sharp), 2340 (w, sharp), 2184 (m, sh, ν_{CN}), 2175 (ms, sh, ν_{CN}), 2167 (ms, ν_{CN}), 2152 (vs, ν_{CN}), 2131 (m, sh, ν_{CN}), 2055 (w, br), 1911 (w, br), 1658 (s, sharp, ν_{CO}), 1496 (ms, m, ν_{N-H}), 1436 (m, sharp, ν_{C-H}), 1419 (m, sh, ν_{C-H}), 1381 (m, s). IR (Nujol mull, ν_{CN}, cm^{-1}): 2152 (s), 2136 (m, sh).

X-ray Structure Determination. Suitable single crystals were mounted and sealed inside glass capillaries of 0.3 or 0.5 mm diameter under N_2. Single-crystal X-ray diffraction data were collected on an Enraf-Nonius CAD4 diffractometer using graphite-monochromated Mo Kα radiation (0.710 73 Å). Unit cell parameters were obtained by a least-squares refinement of the angular settings from 25 reflections, well distributed in reciprocal space and lying in the 2θ range of 24−30°.

The diffraction data were corrected for Lorentz and polarization effects and for absorption correction (empirically from ψ scan data). The structure was solved using the SHELX-97 structure solution package.[23] The Patterson method was employed to locate metal atoms. The remaining of non-hydrogen atoms were located by the Fourier method and refined on F^2 through full-matrix least-squares refinement procedures. After all non-hydrogen atoms were located and refined anisotropically, the hydrogen atoms of DMF molecules were calculated assuming ideal −CH and $-CH_3$ conformation.

Acknowledgment. This work was supported by the National Science Foundation through Grant No. CHE 00115. We thank Dr. Jun Li for help in the interpretation of IR data.

Supporting Information Available: Table of angles for ideal dodecahedron, bicapped trigonal prism, and square antiprism compared with polyhedral angles for **1**, **2**, and **3**, figures, and the FT-IR spectra. Three X-ray crystallographic files, in CIF format, are available. This material is available free of charge via the Internet at http://pubs.acs.org.

IC0014787

(23) SHELXTL97 was used to solve and refine crystal structures from the diffraction data (Siemens Energy & Automation, Inc., Madison, WI, 1994).